Sub-chronic peripheral CB1R inhibition enhances cognitive performance and induces hippocampal synaptic plasticity changes in naïve mice

Araceli Bergadà-Martínez[1], Lucía de los Reyes-Ramírez[1], Sara Martínez-Torres[1], Irene Martínez-Gallego[2], Rafael Maldonado[1,3], Antonio Rodríguez-Moreno[2], Andrés Ozaita[*1,3]

Affiliations

[1]Laboratory of Neuropharmacology-NeuroPhar, Department of Medicine and Life Sciences, Universitat Pompeu Fabra, Barcelona, Spain.

[2]Laboratory of Cellular Neuroscience and Plasticity, Department of Physiology, Anatomy and Cell Biology, University Pablo de Olavide, Seville, Spain.

[3]IMIM Hospital del Mar Research Institute, Barcelona, Spain.

*Corresponding author: Andrés Ozaita, Laboratori de Neurofarmacologia, Facultat de Ciències de la Salut i de la Vida, Universitat Pompeu Fabra, Parc de Recerca Biomèdica de Barcelona, C/Doctor Aiguader 88, 08003 Barcelona, Spain. Phone: +34-93-3160823; Fax: + 34-93-3160901; e-mail: andres.ozaita@upf.edu.

Abstract

The peripheral contribution to brain function and cognitive performance is far from understood. Cannabinoid type-1 receptor (CB1R), a well-recognized player in cognitive function, is classically pictured in the central nervous system to have such a role. Our group previously demonstrated a novel mechanism where the acute peripheral CB1R inhibition in mice promotes low arousal memory persistence. Here, to elucidate the associated synaptic modifications involved, we evaluated the cognitive outcomes as well as cellular and molecular consequences of a sub-chronic treatment with the peripherally-restricted CB1R antagonist AM6545. Sub-chronic AM6545 resulted in enhanced memory persistence in the novel object-recognition memory test in both males and females and also improving emotional memory. In addition, executive function was facilitated after repeated AM6545 administration further strengthening the nootropic properties of peripheral CB1R inhibition. Transcriptional analysis of hippocampal synaptoneurosomes from treated mice revealed changes in the transcript expression of subunit 1 of N-methyl-D-aspartate (NMDA) receptor isoforms. Notably, AM6545 treatment occluded long-term potentiation in hippocampal synapses while enhancing input-output relation. These changes in synaptic plasticity were accompanied by an increase in the hippocampal expression of *Bdnf* and *Ngf* neurotrophic factors. Our results suggest that repeated peripheral CB1R inhibition contributes to the modulation of memory persistence, executive function, and hippocampal synaptic plasticity in mice, further indicating that peripheral CB1R could act as targets for a novel class of nootropic compounds.

Introduction

Most everyday events create low arousal non-emotional memory traces that may fade away or persist through unpredictable periods that may go on for as long as a lifetime (Morris, 2006). The persistence of memory is facilitated in emotional memories, where encoding is intermingled with the natural stress-coping response, leading to a significant enhancement in memory recall for the sensory information encoded at that time (Roozendaal et al., 2009).

The endocannabinoid system (ECS) is an endogenous neuromodulatory system highly expressed in the central nervous system (CNS) and peripheral tissues, and plays a relevant role in modulating learning and memory processes. Cannabinoid type-1 receptor (CB1R) is the most highly expressed G-protein coupled receptor subtype in the CNS. Within the brain is found in high density in regions such as the hippocampus or the cortex, as well as other memory-related regions (Pacher et al., 2006; Zanettini et al., 2011). Besides its high expression in the brain, CB1R is also present in many peripheral tissues such as the liver, adipose tissue, endocrine system, or skeletal muscle. Regarding its cellular distribution, CB1R is detected predominantly at presynaptic sites where it suppresses neurotransmitter release depending on local synaptic activity (Ohno-Shosaku & Kano, 2014). As reported, activation of the CB1R in adrenergic and noradrenergic cells leads to a decrease in the release of adrenaline and noradrenaline (Ishac et al., 1996; Niederhoffer et al., 2001). It has been observed that the administration of CB1R agonists in rodents is related to memory deficits in several memory types such as recognition memory (Puighermanal et al., 2009), spatial memory (Da Silva & Takahashi, 2002) or fear memory (Kruk-Slomka & Biala, 2016; Pamplona & Takahashi, 2006). On the contrary, CB1R antagonists prevented some of these memory impairments (Barna et al., 2007; Pamplona & Takahashi, 2006). Interestingly, it was previously demonstrated that the

acute inhibition of peripheral CB1R from dopamine β-hydroxylase (DBH+) cells from adrenal glands triggers an adrenergic mechanism that derives in an enhancement in memory persistence that involves the vagus nerve. This cognitive enhancement is accompanied by changes in functional brain connectivity as well as an increase in hippocampal extracellular noradrenaline (Martínez-Torres et al., 2023).

In the present study, we have investigated the impact of the sub-chronic peripheral CB1R inhibition in both emotional and non-emotional memory and the neurobiological mechanisms involved. For this purpose, we have used a combination of behavioral tests, transcriptomic, electrophysiological and biochemical studies. We found that sub-chronic peripheral CB1R inhibition results in enhanced cognitive performance in both male and female mice. Moreover, we reported synaptic plasticity modifications in the hippocampus after the treatment, including differential expression of N-methyl-D-aspartate (NMDA) receptor 1 isoforms, modulation of hippocampal long-term potentiation and enhanced expression of neurotrophic factors. These central effects of repeated peripheral CB1R inhibition unmask a target worth exploring in the context of cognitive improvement.

Materials and methods

Ethics

All animal procedures were conducted following "Animals in Research: Reporting Experiments" (ARRIVE) guidelines and standard ethical guidelines (Kilkenny et al., 2010) (European Directive 2010/63/EU). Animal procedures were approved by the local ethical committee (Comitè Ètic d'Experimentació Animal-Parc de Recerca Biomèdica de Barcelona, CEEA-PRBB).

Animals

Young adult (8-12 weeks old) male and female Swiss albino (CD-1) and C57BL/6J mice (Charles River) were used for pharmacological approaches on behavioral, transcriptomic, electrophysiological and biochemical experiments. Mice were housed in Plexiglas cages (2-4 mice per cage in the case of males and 2-5 in the case of females) and maintained in temperature (21 ± 1 °C) and humidity (55 ± 10%) controlled environment. Food and water were available *ad libitum*. Animals tested in the touchscreen apparatus were food-restricted to 85-95% of their free-feeding weight beginning 3 days before pre-training. These mice were maintained on food restriction for the entire experiment although daily food allowance increased over time to prevent stunting. All the experiments were performed during the light phase of a 12 h cycle (light on at 8 am; light off at 8 pm). Mice were habituated to the experimental room and handled for 1 week before starting the experiments. All behavioral experiments were conducted by an observer blind to experimental conditions.

Drugs and treatments

AM6545 (Tocris-Bio-Techne) was dissolved in 0.26% DMSO, 4.74% ethanol, 5% cremophor-EL and 90% saline. Sotalol (Sigma-Aldrich) was dissolved in saline

(Martínez-Torres et al., 2023). All drugs were injected intraperitoneally (i.p.) in a volume of 10 mL/kg of body weight. AM6545 was administered at the dose of 1 mg/kg and sotalol at the dose of 10 mg/kg. Sub-chronic administrations consisted on 7 days of treatment. For the pairwise discrimination acquisition, AM6545 was administered 30 min after the end of the pairwise discrimination session every day until the experiment finished.

Novel object-recognition test

Novel object-recognition test (NORT) was performed as previously described (Martínez-Torres et al., 2023). Briefly, on day 1 mice were habituated to a V-shaped maze (V-maze) for 9 min. On day 2 (training phase), two identical objects (familiar objects) were located at the end of each corridor and mice were left to explore them for 9 min. To assess memory persistence, the test phase, also of 9 min, was performed 48 h later, and one of the familiar objects was replaced by a new object (novel object). The time spent exploring each of the objects was computed to calculate a discrimination index (DI = (Time Novel Object - Time Familiar Object)/(Time Novel Object + Time Familiar Object)). Object exploration time was considered when the orientation of the nose was towards the object. A higher discrimination index is considered to reflect greater memory retention for the familiar object. Importantly, in this work a variation of this protocol was applied when required, which consisted on a reduction in the training phase to 3 min and performing the test phase 24 h later. These two versions of the task allow assessing memory under challenging conditions. For this task, drug treatment was administered after the training phase in sub-chronic treatments. For the measurement of the effects after treatment withdrawal the treatment finished 24 h prior to the training phase.

Novel place-recognition test

On days 1 and 2 mice were introduced into an empty arena (25x25x15 cm) with spatial cues and dimly illuminated (2-3 lux), and were allowed to freely explore it during 9 min (habituation phase). On day 3, two identical objects were positioned in opposite corners (familiar location) (6 cm away from the walls) and mice were allowed to explore them during 9 min (training phase). 48 h later, mice were introduced in the same arena with the same objects, but one of them was moved to a new location (novel location) (another corner, 6 cm away from the walls). Mice were allowed to explore the objects for 9 min (test phase). The time spent exploring each of the objects was computed to calculate a discrimination index (DI = (Time Novel Location - Time Familiar Location)/(Time Novel Location + Time Familiar Location)). Object exploration time was considered when the orientation of the nose was towards the object. A higher discrimination index is considered to reflect greater memory retention for the familiar location.

Emotional memory persistence assessment in the context fear conditioning

Context fear conditioning (FC) was used to measure the effect of AM6545 on hippocampal-dependent emotional memory in mice. On day 1, mice were placed in a conditioning chamber with an electrifiable floor. After 3 min of free exploration, mice received one footshock (unconditioned stimulus, US: 2 sec, 0.35 mA intensity) (training phase). On day 2 (first extinction session), 24 h after the training phase, mice were placed for 5 min in absence of the footshock in the same conditioning chamber and the freezing behavior was manually recorded. Extinction sessions (Ext1-Ext5) were performed at 24, 48, 96, 72 and 96 h after the footshock, and freezing behavior was manually counted. Treatment with AM6545 was administered immediately after each extinction session.

Elevated plus maze test

The elevated plus maze test was performed as previously described (Navarro-Romero et al., 2022). The test consisted of a black Plexiglas apparatus with four arms (29 cm long ×

5 cm wide) set in cross from a neutral central square (5 cm × 5 cm) elevated 40 cm above the floor. Five-minute test sessions were performed after 7 days of treatment 24 h after the last AM6545 or vehicle administration, and the percentage of time and entries in the open arms were determined.

Locomotor activity

Locomotor activity was assessed for 30 min after 7 days of treatment 24 h after the last drug administration as previously described (Navarro-Romero et al., 2022). Individual locomotor activity boxes (9 × 20 × 11 cm) (Imetronic) were used in a low luminosity environment. The number of horizontal movements was detected by a line of photocells located 2 cm above the floor.

Touchscreen apparatus

Automated touchscreen operant systems (Campden Instruments) were used to test learning (Horner et al., 2013). The system was controlled by ABET II software (Campden Instruments). Mice began the experiment at 8-12 weeks of age and were tested in the same chamber daily five days a week until the end of the experiment.

Pairwise discrimination task

Mice were habituated to the chamber prior to pre-training and testing. During habituation, the mouse is left in the chamber during 20 min. A tone was played and the reward magazine illuminated indicating the delivery of 10% condensed milk (CM) (150 µl). After a nosepoke there was a 10 s delay before a tone was played, the reward magazine illuminated again and CM was then delivered (7 µl). The procedure was repeated until the session ended. Following habituation, mice started the pre-training that consisted on four different stages. Each session lasted a maximum of 60 min. On stage 1, images/stimuli were displayed one at a time on one side of the touchscreen. The other

side remained blank. Trials resulted in the delivery of the CM either upon touching the image or after an intertrial interval (ITI) of 20 s, whichever came first. On stage 2, the reinforcement was only delivered if mice touched the image. Mice remained in this stage until they performed 30 trials in a session. On stage 3, mice had to enter the reward magazine to initiate each trial. Mice remained in this stage until they performed 30 trials in a session. On stage 4, if mice touched the blank side of the touchscreen the house light illuminated for a time out period (5 s) and no reward was given. Mice remained in this stage until they performed 23 correct trials out of 30 in a session. Finally, in the pairwise discrimination acquisition, mice were taught to discriminate and choose a rewarded image (S+) over an unrewarded image (S-). The two images were randomly presented on the right or left side of the touchscreen. Touching the correct stimulus resulted in the delivery of the reward, whereas touching the incorrect stimulus resulted in the illumination of the house light. An incorrect trial led to a correction trial in which the two images were presented in the same location as in the previous trial. Correction trials were not included in the final correct trials count. Mice completed the task when they performed 24 correct trials out of 30 (80%) for two days in a row. Animals that did not achieve the goal within 20 sessions were excluded from the experiment (Four animals were excluded, one vehicle-treated and three AM6545-treated).

Tissue preparation for mRNA and biochemical analysis

Mice were treated with AM6545 (1 mg/kg, i.p.) or vehicle for 7 days. 24 h after the last administration, hippocampal and cortical tissues were dissected on ice, frozen on dry ice and stored at -80 ºC until used.

Tissue preparation for RNA extraction

Synaptoneurosome preparation: for RNA of a synaptoneurosome-enriched fraction, synaptoneurosome preparation was performed as previously described (Salgado-

Mendialdúa et al., 2018). Hippocampal tissue was dounce-homogenized by 10 strokes with a loose pestle and 10 strokes with a tight pestle in 30 volumes of ice-cold synaptoneurosome lysis buffer (in mM: 2.5 CaCl2, 124 NaCl, 3.2 KCl, 1.06 KH2PO, 26 NaHCO3, 1.3 MgCl2, 10 Glucose, 320 Sucrose, 20 HEPES/NaOH pH7.4) including phosphatase inhibitors (in mM: 5 NaPyro, 100 NaF, 1 NaOrth, 40 beta-glycerolphosphate) and protease inhibitors (1 µg/mL leupeptin, 10 µg/mL aprotinin, 1 µg/mL pepstatin and 1 mM phenylmethylsulfonyl fluoride). This crude homogenate was centrifuged for 1 min at 2,000 g, 4 °C, and the supernatant was recovered (S1). The pellet was resuspended in 1 mL of synaptoneurosome lysis buffer for further centrifugation (1 min at 2,000 g, 4 °C). This second supernatant (S2) was recovered and combined with S1. Total supernatant (S1 + S2) was passed through a 10 µm hydrophobic PTFE filter (LCWP02500, Merck Millipore) and centrifuged for 1 min at 4,000 g, 4 °C to attain the supernatant (S3). S3 was transferred to a new tube and centrifuged for 4 min at 14,000 g, 4 °C. This final supernatant (S4) was discarded and the pellet was used as the synaptoneurosomal fraction. Subsequent RNA extraction was performed using a RNeasy Mini kit (74140, QIAGEN) according to the manufacturer's instructions.

Total homogenate: for RNA of total hippocampal homogenates, hippocampal tissue was dounce-homogenized using a RNeasy Mini kit (74140, QIAGEN) according to the manufacturer's instructions.

Hippocampal synaptoneurosomal RNA Sequencing

mRNA libraries from C57BL/6J male mice (VEHICLE, n = 5; AM6545, n = 5) were obtained by Macrogen Inc. using SMARTer Ultra Low Input kit (634940, Takara Bio/Clontech). All samples were sequenced in parallel using Illumina NovaSeq 6000 flow cell and fastq files have been deposited on the Gene Expression Omnibus (GEO) database (GSE245307). Reads were aligned to Ensembl GRCm39 annotations to quantify

transcript abundance using Salmon 1.5.2 (Patro et al., 2017) and tximport (v1.18) R package (Soneson et al., 2016). For differential expression analysis, DESeq2 (v1.30) (Love et al., 2014) was performed in R environment (v4.0) using both gene and transcript level. Significance cut-off was set on a |log2fold change| > 0 and based on adjusted p-value < 0.1 for genes or adjusted p-value < 0.05 for transcripts. Finally, functional enrichment analysis was performed using clusterProfiler (v3.14) Bioconductor package (Yu et al., 2012), in which statistically significance was defined based on adjusted p-value < 0.05 for each gene ontology enriched term.

Reverse transcription

RNA concentration and integrity was measured using an Agilent 2100 Bioanalyzer (Agilent Technologies). Reverse transcription was performed in similar amounts of RNA to produce cDNA in a 20 µl reaction using the High Capacity cDNA Reverse Transcription kit (Applied Biosystems) according to the manufacturer's instructions.

Quantitative real-time PCR analysis

Real-time PCR was carried out in a 10 µl reaction using 0.1 ng/µl of cDNA, using SYBR Green PCR Master Mix (Roche) according to the manufacturer's protocol with a QuantStudio 12 K Flex Real-Time PCR System (Applied Biosystems).

Quantification was performed using the comparative CT Method (ΔΔCT Method). All the samples were tested in triplicate and the relative expression values were normalized to the expression value of β-actin (for total gene expression analysis), or to β2-microglobulin or the mean of *Grin1* common and β2-microglobulin (for *Grin1* isoforms expression analysis). The fold change was calculated using the eq. 2(–ΔΔCt) formula, as previously reported (Livak & Schmittgen, 2001). The following primers specific for mouse were used:

Gene	Forward	Reverse
Bdnf	CAGGTGAGAAGAGTGATGACC	ATTCACGCTCTCCAGAGTCCC
Ngf	CAAGGACGCAGTTTCTATACTG	CTTCAGGGACAGAGTCTCCTTCT
Actb	CGTGAAAAGATGACCCAGATCA	CACAGCCTGGATGGCTACGT
Grin1 common	CATCATCTCAAACCAGACGCT	CTGACTACCCGAATGTCCATC
Grin1 exon 5 (NR1(1-4)b)	GCAGAGCCGTCACATTCTT	ACCTCGACCAACTGTCCTAT
Grin1 exon 4-6 (NR1(1-4)a)	ATGCGCGTCTACAACTGG	ACATTCTTGGTTCCTGGGTC
B2m	TTCTGGTGCTTGTCTCACTGA	CAGTATGTTCGGCTTCCCATTC

Ex vivo electrophysiological recordings in the hippocampus

Hippocampal slices were prepared as described in detail elsewhere (Falcón-Moya et al., 2021; Pérez-Rodríguez et al., 2019). Briefly, mice were anesthetized with isoflurane (2% v/v) and brains were rapidly removed into ice-cold solution (I) consisting of (in mM): 126 NaCl, 3 KCl, 1.25 KH2PO4, 2 MgSO4, 2 CaCl2, 26 NaHCO3, and 10 glucose (pH 7.2, 300 mOsmL-1), and positioned on the stage of a vibratome slicer and cut to obtain transverse hippocampal slices (350 mm thick), which were maintained continuously oxygenated for at least 1 h before use. All experiments were carried out at physiological temperature (30–34 ºC). For experiments, slices were continuously perfused with the solution described above.

For LTP studies, whole-cell patch-clamp recordings were made from pyramidal cells located in the CA1 field of the hippocampus. CA1 pyramidal cells were patched under visual guidance by infrared differential interference contrast microscopy and verified to be pyramidal neurons by their characteristic voltage response to a current step protocol. Neurons were recorded using the whole-cell configuration of the patch-clamp technique in voltage-clamp mode with a patch-clamp amplifier (Multiclamp 700B), and data were acquired using pCLAMP 10.2 software (Molecular Devices). Patch electrodes were pulled from borosilicate glass tubing and had resistances of 4–7 MΩ when filled with (in mM): CsCl, 120; HEPES, 10; NaCl, 8; MgCl2, 1; CaCl2, 0.2; EGTA, 2 and QX-314, 20

(pH 7.2–7.3, 290 mOsm L−1). Cells were excluded from analysis if the series resistance changed by more than 15% during the recording.

In paired-pulse experiments, 2 consecutive stimuli separated by 40 ms were applied at the beginning of the baseline recording and again 30 min after applying the LTP protocol. Data were filtered at 3 kHz and acquired at 10 kHz. A stimulus-response curve (1–350 μA, mean of 5 excitatory postsynaptic current, EPSC, determination at each stimulation strength) was compiled for each experimental condition. Paired-pulse ratio (PRR) was expressed as the amplitude of the second response (EPSC) divided by the amplitude of the first (Falcón-Moya et al., 2021). Data were analyzed using the Clampfit 10.2 software (Molecular Devices). The last 5 min of recording was used to estimate changes in synaptic efficacy compared to baseline.

Tissue preparation for immunoblot analysis

For obtaining total hippocampal homogenates, hippocampal tissue was dounce-homogenized by 20 strokes with a loose pestle and 20 strokes with a tight pestle in 30 volumes of ice-cold lysis buffer (50 mM Tris-HCl pH 7.4, 150 mM NaCl, 10% glycerol, 1 mM EDTA, 1 μg/mL aprotinin, 1 μg/mL leupeptine, 1 μg/mL pepstatin, 1 mM phenylmethylsulfonyl fluoride, 1 mM sodium orthovanadate, 100 mM sodium fluoride, 5 mM sodium pyrophosphate, and 40 mM beta-glycerol phosphate) and 1% Triton X-100 using a Dounce homogenizer. After 10 min incubation at 4 ºC, samples were centrifuged at 16,000 g for 30 min to remove insoluble fragments. Protein content in the supernatants was determined by DC-micro plate assay (Bio-Rad), following manufacturer's instructions. Equal amounts of brain lysates were separated in 10% SDS-polyacrylamide gels before electrophoretic transfer onto nitrocellulose membrane overnight at 4 ºC. Nitrocellulose membranes were blocked for 1 h at room temperature in Tris-buffered saline (TBS) (100 mM NaCl, 10 mM Tris, pH 7.4) with 0.1% Tween-20 (T-TBS) and 3%

bovine serum albumin. Afterwards, nitrocellulose membranes were incubated for 2 h with the primary antibodies. Anti-BDNF (mouse, 1:150, 327-100, Icosagen) and anti-actin (mouse, 1:20,000, MAB1501, Millipore) were used as primary antibodies. Then, nitrocellulose membranes were washed 3 times (5 min each) and subsequently incubated with the corresponding secondary antibody for 1 h at room temperature. Anti-rabbit (1:15,000, 7074S, Cell Signaling) or anti-mouse (1:15,000, 7076S, Cell Signaling) were used as secondary antibodies. After 3 washes (5 min each), immunoreactivity was visualized by enhanced chemiluminescence detection (Luminata Forte, Amersham). Optical densities of relevant immunoreactive bands were quantified after acquisition on a ChemiDoc XRS System (Bio-Rad) controlled by The Quantity One software v 4.6.9 (Bio-Rad). For quantitative purposes, the optical density values were normalized to β-actin values in the same sample and were expressed as a percentage of control treatment.

Tissue preparation for immunofluorescence

Mice were deeply anesthetized by i.p. injection (0.2 mL/10 g of body weight) of a mixture of ketamine/xylazine (100 mg/kg and 20 mg/kg, respectively) prior to intracardiac perfusion of cold 4% paraformaldehyde in 0.1 M phosphate buffer, pH7.4 (PB). Brains were removed and post-fixed overnight at 4 °C in the same fixative solution. The next day, brains were moved to PB at 4 °C. Coronal brain sections of 30 µm were made on a freezing microtome (Leica SM 2000) and stored in a 5% sucrose solution at 4 ºC until use.

Ki67 immunofluorescence and cell quantification

Immunofluorescence and cell quantification were performed as previously described (Navarro-Romero et al., 2019). Brain sections were washed thrice with PB and blocked with 3% normal donkey serum and 0.3% Triton X-100 in PB (NDS-T- PB) at room temperature for 2 h. Slices were incubated overnight in the NDS-T- PB with the primary

antibody to Ki67 (rabbit, 1:300, ab15580, Abcam). The next day, sections were washed three times in PB and incubated at room temperature with the secondary antibody to rabbit immunoglobulins (rabbit, Alexa Fluor-488, A21206, 1:600, Life Technologies) in NDS-T- PB for 2 h at room temperature. After incubation, sections were rinsed thrice with PB and then mounted onto glass slides coated with gelatine, in Fluoromount-G with DAPI (Thermo Fisher Scientific) as mounting medium.

Images of stained sections were obtained with a confocal microscope TCS SP5 LEICA (Leica Biosystems) using a dry objective (20×) with a sequential line scan at 1024 × 1024 pixel resolution. The images were obtained choosing a representative 10 µm Z-stack from the slice. The density of positive cells was quantified manually over the projection visualized after the application of an optimal automatic threshold (MaxEntropy) from Fiji software (ImageJ). The number of positive cells was calculated as the mean of total number of cells counted referred to the volume of the SGZ (µm3). Positive cells density was referred to that calculated for the control group.

Statistical analysis

Results are reported as mean ± standard error of the mean (s.e.m). Data analyses were performed using GraphPad Prism software (GraphPad Prism 8). Statistical comparisons were evaluated using unpaired Student's t-test for 2 groups comparisons or two-way ANOVA for multiple comparisons. Subsequent Bonferroni *post hoc* was used when required (significant interaction between factors). All results were expressed as mean ± s.e.m. Comparisons were considered statistically significant when $p < 0.05$.

Results

Repeated AM6545 treatment enhances novel object, place recognition and fear memory

We performed a sub-chronic treatment with AM6545 for 7 days to assess whether tolerance to the mnemonic effects of acute AM6545 previously described (Martínez-Torres et al., 2023) was developed after repeated treatment. We tested memory at 48 h as we previously demonstrated that object-recognition memory is significantly reduced at this time point after training, which makes it a suitable interval to assess memory persistence (Martínez-Torres et al., 2023). We observed that sub-chronic AM6545 treatment potentiated memory recall at this time point in the NORT in both male (Student's t-test: $p = 0.002$) (Figure 1A) and female (Student's t-test: $p = 0.001$) mice (Figure 1B), indicating the lack of tolerance to the mnemonic effect of AM6545. We next reduced the time of the training phase from 9 min to 3 min. 24 h later, we tested memory and we observed that AM6545 improved memory performance in both male (Student's t-test: $p = 0.0023$) (Figure 1C) and female (Student's t-test: $p = 0.005$) mice (Figure 1D), thus indicating that the peripheral CB1R inhibition also enhances memory performance under these conditions suggesting a facilitation in memory consolidation under two different challenging conditions. To assess the permanency of AM6545 effects in the NORT, we next performed the task after sub-chronic treatment withdrawal. Under these conditions, we still observed an enhancement in memory performance (Student's t-test: $p = 0.029$) (Figure 1E), suggesting a standing effect of repeated treatment with AM6545 over relevant cognitive brain areas. We have previously reported that pretreatment with a single administration of the peripheral β-adrenergic blocker sotalol, prevents the mnemonic effect of acute AM6545 (Martínez-Torres et al., 2023). Here, we administered sotalol during 7 days 20 min before each administration of AM6545 to assess if this peripheral adrenergic mechanism is also involved in the repeated effect of AM6545. We

observed that sotalol pretreatment prevented the procognitive effects of AM6545 in the NORT (two-way ANOVA, interaction: F (1,52) = 7.993, p = 0.006; post hoc Bonferroni, Saline-VEH vs Saline-AM6545 p = 0.0014; Saline-AM6545 vs Sotalol-AM6545 p = 0.0018) (Figure 1F), indicating the participation of an adrenergic mechanism in the action of AM6545.

Additionally, we assessed if the repeated exposure to AM6545 was able to improve spatial memory persistence in the novel place recognition test (NPRT). When we tested memory at 48 h after the training phase, the sub-chronic AM6545 treatment showed an enhancement in spatial memory persistence (Student's t-test: p = 0.049) (Figure 1G), pointing to a role in modulating also spatial memory. It was previously observed that systemic inhibition of CB1R increases anxiety-like behavior in rodents (Patel and Hillard, 2006). In order to evaluate the effect of the peripheral CB1R antagonist on anxiety-like behavior we performed the elevated plus-maze test after 7 days of treatment. We observed that the percentage of time and entries to the open arms did not significantly change (Supplementary Fig. 1A-B) compared to vehicle-treated mice, indicating that AM6545 at a dose of 1 mg/kg is not producing an unspecific effect in the anxiety-like response. We also assessed locomotor activity in actimeter boxes after sub-chronic administration of the peripheral CB1R antagonist AM6545. Similarly, we found no significant effect of AM6545 in the locomotor activity as reflected in total activity and rearings measurements (Supplementary Fig. 1C-E).

Next, we studied whether peripheral CB1R inhibition would modify memory persistence in an emotional task using the context fear conditioning paradigm, by administering AM6545 (1 mg/kg, i.p.) after each extinction session. We observed that AM6545-treated mice prevented fear extinction across extinction sessions (Ext2-Ext5) (two-way repeated measures ANOVA, treatment effect: F (4,75) = 3.178, p = 0.018; post hoc Bonferroni,

Ext3-VEH vs Ext3-AM6545, $p = 0.024$, Ext4-VEH vs Ext4-AM6545, $p = 0.017$, Ext5-VEH vs Ext5-AM6545, $p = 0.003$) (Figure 1H).

Long-term treatment with AM6545 improves executive function in the pairwise discrimination task

To test whether the peripheral CB1R inhibition is affecting executive function we performed the pairwise discrimination task using the touchscreen chambers with previously validated images (Figure 2A) (Boyers et al., personal communication). We administered AM6545 every day after the pairwise discrimination session until mice completed the task. We observed that AM6545-treated mice showed a more rapid learning compared to vehicle as reflected in a smaller number of correction trials (Student's t test: $p = 0.001$), and a reduced number of sessions to complete the task (Student's t test: $p = 0.026$) (Figure 2B-C). There was a non-significant (Student's t-test: $p = 0.10$) trend for AM6545-treated mice to perform less trials to reach criterion (Figure 2D). We also analyzed other control parameters such as the reward collection latency, the correct and incorrect touch latency, the left and right intertrial interval (ITI) touches and the time to initiate the trials. No significant differences in any of these parameters were observed (Supplementary Fig. 2A-F). There were also no significant changes in the body weight variation (Δbody weight) between groups during the protocol (Supplementary Fig. 2G), altogether indicating no major changes in general activity produced by AM6545.

Hippocampal synaptoneurosome transcriptomic analysis after sub-chronic peripheral CB1R inhibition

We were interested in studying the potential synaptic modifications associated with the procognitive effect produced by AM6545. For this, we first used RNA sequencing to perform gene expression profile of five male mice sub-chronically treated with vehicle and five male mice sub-chronically treated with AM6545 at a dose of 1 mg/kg. As we

wanted to evaluate synaptic modifications promoted by peripheral CB1R modulation, we focused on hippocampal synaptoneurosomal enriched fractions (Salgado-Mendialdúa et al., 2018). When we analysed gene expression, few genes appeared differentially expressed, including *Sinhcaf*, *Sned1*, *Ccl21b*, *Exosc6* and *Otud7b* (Supplementary Figure 3). Assuming that synaptic contacts are fractions with local translation and with high abundance in transcript content, we also analysed differential expression at transcript level (Hafner et al., 2019). We found that 278 transcripts were differentially modulated in AM6545 treated male mice compared with vehicle (Figure 3A). In fact, with an adjusted p-value < 0.05, 133 transcripts were upregulated while 145 transcripts were downregulated (AM6545 *vs.* VEHICLE). Overall, these results show that AM6545 modulation in synaptoneurosome enriched fractions was more sensitive when the analysis was performed at transcript level rather than gene level. Regarding gene ontology analysis, we observed that upregulated transcripts present an enrichment in terms related with synapse structure and activity and pre- and post-density localization (Figure 3B). However, downregulated transcripts seem less associated between them as we obtained more specific molecular functions such as methyltransferase activity or catalytic processes (Figure 3C). Interestingly, we found that gene ontology terms associated with synapses were in common among up- and downregulated transcripts, showing the possible preferential involvement of specific transcripts from the same gene based on treatment. To decipher this extent, we performed an overlap analysis between up and downregulated transcripts regarding its parent gene, and we found that four genes (*Grin1*, *Elavl4*, *Sorbs1* and *Golga2*) preferentially expressed different transcripts depending on AM6545 or vehicle administration (Figure 3D). From all these genes, *Grin1* encodes subunit 1 of the N-methyl-D-aspartate (NMDA) receptor (NMDA-NR1), an essential glutamate-gated calcium ion channel with key role in synaptic function (Sengar et al.,

2019). This gene can generate eight splicing variants that leads to the expression of eight isoforms (four isoforms a -NR1-1a to NR1-4a- and four isoforms b - NR1-1b to NR1-4b-), each of them with different functionality (Flores-Soto et al., 2013). We will refer to isoforms a as NR1(1-4)a and to isoforms b as NR1(1-4)b. In fact, in AM6545 treated male mice we observed the upregulation of transcript ENSMUST00000114318 that encodes for isoform NR1-3a, and the downregulation of transcript ENSMUST00000114310 that encodes NR1-1a isoform (Figure 3E). To further explore the modulation of *Grin1* isoforms, we measured by quantitative RT-PCR the differential mRNA expression of *Grin1* isoforms. This analysis included *Grin1* common domain (expressed by all eight isoforms), *Grin1* exon 5 (expressed in NR1(1-4)b isoforms that include N1 cassette) and *Grin1* exon 4-6 (expressed in NR1(1-4)a isoforms, that exclude N1 cassette) (Figure 4A). As expected from *in silico* gene expression analysis, we observed no significant changes in *Grin1* common domain (Student's t-test: $p = 0.528$) (Figure 4B). However, a significant decrease was observed in *Grin1* exon 5 in mice treated with AM6545 (Student's t-test: $p = 0.014$) (Figure 4C) but such a modulation was not observed in *Grin1* exon 4-6 (Figure 4D), suggesting a global change in isoforms b but not in isoforms a. Next, we investigated if some of these changes were also reproducible in synaptoneurosomes from the cortex, as it is another brain area related with cognition. We repeated the same analysis and assessed the same isoforms. No significant changes were observed in *Grin1* common (Figure 4E). Interestingly, as in the hippocampus, a significant *Grin1* exon 5 decrease was observed in AM6545-treated mice compared to vehicle (Student's t-test: $p = 0.0024$) (Figure 4F) and again *Grin1* exon 4-6 expression was not modulated (Figure 4G). However, when we analyzed these *Grin1* isoforms from female hippocampal synaptoneurosomes, we observed no significant changes in neither of them (Supplementary Figure 4), pointing to sex differences in *Grin1* modulation by AM6545.

Sub-chronic AM6545 treatment induces synaptic plasticity changes in the hippocampus

To investigate the functional consequences of peripheral CB1R inhibition in hippocampal plasticity, we studied LTP at Schaffer collateral-CA1 synapses in slices from mice treated for 7 days with AM6545 (1 mg/kg) or vehicle. Acute hippocampal slices were obtained 24 h after the last drug administration, the time when novel object-recognition memory assessment and transcriptomic analyses were performed. LTP was induced by stimulating Schaffer collaterals at 100-Hz during 1s. Slices from vehicle-treated mice showed robust LTP (168 ± 10 %), whereas LTP was completely occluded in slices from mice treated with AM6545 (96 ± 8 %) (Student's t-test: $p = 0.002$) (Figure 5A-B). To determine the site of expression of LTP, we analyzed pair-pulse ratios during baseline and 30 min after LTP induction. This analysis showed no differences in control slices (1.41 ± 0.11 after LTP vs 1.67 ± 0.16 in baseline) (Figure 5C) confirming the established postsynaptic expression of this form of LTP. Repeated treatment with AM6545 did not induce changes in PPR (1.51 ± 0.18 after LTP vs 1.89 ± 0.17 in baseline). We also compiled a stimulus-response curve (50-350 µA) to examine whether the basal synaptic transmission would be modified in mice treated with AM6545 for 7 days. We found that slices from AM6545-treated mice presented increased amplitude of EPSCs (Figure 5D).

Next, we evaluated the expression of neurotrophic factors in the hippocampus to assess the mechanism involved in AM6545 effect on synaptic plasticity. Quantitative RT-PCR analysis showed a significant enhancement in the mRNA levels of *Ngf* (Student's t-test: $p = 0.018$) (Figure 5E) and *Bdnf* (Student's t-test: $p = 0.009$) (Figure 5F) after sub-chronic 7 days AM6545 treatment. Interestingly, immunoblot analysis supported the increase of BDNF levels in hippocampal homogenates of mice treated for 7 days with AM6545 (Student's t-test: $p = 0.009$) (Figure 5G).

We also assessed whether sub-chronic AM6545 treatment produces proliferation of neuronal precursors in the hippocampus. Adult neurogenesis was studied through the quantification of the number of cells expressing the endogenous marker of cell proliferation Ki67 in the subgranular zone (SGZ) of the dentate gyrus. Sub-chronic treatment with AM6545 did not significantly modify the number of Ki67+ cells, suggesting that AM6545 is not affecting synaptic plasticity by modulating hippocampal neurogenesis (Supplementary Fig. 5).

Discussion

In this study we reveal a relevant effect of peripheral CB1R inhibition in enhancing memory persistence and facilitating learning, as well as executive function in mice. Such cognitive improvements were accompanied by modifications in NMDA receptor NR1 subunits transcript splicing, modifications in hippocampal synaptic plasticity and changes in hippocampal neurotrophin expression.

Previous studies showed that CB1R systemic antagonists could produce memory improvement (Takahashi et al., 2005; Terranova et al., 1996; Wolff & Leander, 2003). In addition, genetic downregulation of CB1R also enhances memory performance (Maccarrone et al., 2002; Martínez-Torres et al., 2023; Reibaud et al., 1999). This evidence pointed to CB1R as a potential target in memory modulation. In the present study we assessed the cognitive effects of a sub-chronic administration of a peripherally-restricted CB1R antagonist. Here, we demonstrated that no tolerance develops after repeated treatment as object-recognition memory persistence was significantly enhanced in both male and female mice when the test was performed 48 h after training. We used the period of 48 h as we previously revealed that at this time point control mice naturally show reduced novel object discrimination and hence low discrimination indexes (Martínez-Torres et al., 2023). Moreover, we also observed that the repeated AM6545 treatment improved learning in both sexes when NORT was modified by reducing the training period to 3 min, compared to the 9 min in standard conditions. Under these challenging conditions AM6545-treated mice exhibited higher discrimination indexes than control mice, indicating that the treatment is enhancing memory persistence in different challenging settings. Similar to our findings, the reduction of the training period in the NORT has been previously used to assess memory enhancement through exercise in mice (Butler et al., 2019). Additionally, we assessed recognition memory performance

in the NORT after treatment withdrawal, thus the drug was not onboard during memory consolidation. Sub-chronic AM6545 treatment enhanced memory persistence under these conditions, suggesting that the memory improvement could be mediated by persistent brain plasticity changes elicited by the repeated treatment.

Our previous research showed that AM6545-memory improvement after a single administration was dependent on an adrenergic mechanism given that AM6545 mnemonic effect was prevented by the peripherally restricted β-adrenergic antagonist sotalol (Martínez-Torres et al., 2023). The fact that here sotalol pretreatment significantly reduced the mnemonic effect of sub-chronic AM6545 points to a relevant role of the peripheral adrenergic tone. In this regard, the release of adrenaline and noradrenaline from the adrenal glands has a significant effect on memory retention (McIntyre et al., 2012; Yang et al., 2013). In addition, blocking peripheral adrenergic receptors prevented the improvement in memory retention elicited by novelty in a fear conditioning paradigm (King & Williams, 2009), further supporting an adrenergic mechanism involved in memory consolidation which we find could exquisitely involve peripheral CB1R.

We also assessed whether other memory types could be sensitive to this pharmacological intervention with AM6545. We found a significant enhancement in the NPRT, a type of spatial memory, after sub-chronic peripheral CB1R inhibition. Previous work has found that CB1R inhibition with the systemic CB1R antagonist AM281 improves spatial learning in the Morris water maze test in mice with traumatic brain injury (Xu et al., 2019). In this regard, spatial memory deficits induced by the cannabinoid receptor agonist Δ9-tetrahydrocannabinol were prevented by blocking systemic CB1R with rimonabant (Da Silva & Takahashi, 2002). To the best of our knowledge, the results reported herein are the first to point to a potential role of the peripheral CB1R in the improvements of spatial memory performance in naïve young adult mice.

Regarding emotional memory, we reported that a single administration of AM6545 after the first extinction session in the context fear conditioning, promoted freezing behavior when memory was assessed the next day. However, freezing behavior was reduced when assessed during the subsequent extinction sessions (Martínez-Torres et al., 2023). In the present study, we showed that administering AM6545 after every extinction session maintains high freezing levels across days, pointing to a persistent effect of the repeated exposure to AM6545 in emotional memory. This finding is reminiscent of the results obtained with systemic approaches such as the use of the CB1R antagonism rimonabant or the use of CB1R KO mice (Marsicano et al., 2002) that showed significant enhancements in fear memory.

Remarkably, we found that mice that received the repeated AM6545 administration had a better performance in the pairwise discrimination task. In this regard, the use of a systemic CB1R agonist impaired performance in another executive function-related task whereas the administration of a systemic CB1R antagonist prevented this impairment (Arguello & Jentsch, 2004), but the overall effect of the systemic CB1R antagonists on each own was not assessed in the study. Here, we reported that the administration of a peripherally-restricted CB1R antagonist improves executive function, as reflected in the number of correction trials and sessions to criterion in the pairwise discrimination task.

The transcriptomic analysis in a synaptoneurosomal fraction of the hippocampus showed a very limited number of changes at the gene expression level. Instead, when all possible transcripts detected in high-throughput analysis were considered independently, more specific modifications between treatment conditions were revealed. Among those alterations, *Grin1* transcript changes called our attention due to the central role NMDA receptors have in learning, memory and synaptic function (Lau & Zukin, 2007). The NR1 subunit, encoded by *Grin1* gene, is essential for all NMDA receptors and can lead to eight

different isoforms by alternative splicing (NR1(1-4)a and NR1(1-4)b). NR1(1-4)a isoforms differ from NR1(1-4)b isoforms in the absence of an additional extracellular 21-aminoacid stretch encoded by exon 5 (known as the N1 cassette) (Paoletti et al., 2013). Our RT-PCR analysis showed that NR1(1-4)b isoforms were downregulated in the hippocampus and cortex of AM6545-treated mice. Interestingly, previous studies found that LTP was lower in magnitude in mice compulsorily expressing exon 5-encoded N1 cassette (i.e., mice expressing only NR1(1-4)b isoforms) compared to mice lacking from this exon (i.e., mice expressing only NR1(1-4)a isoforms), suggesting that including this exon 5 in the NR1 subunit acts as a damper that suppresses the magnitude of LTP (Sengar et al., 2019). Regarding NR1(1-4)a isoforms, a downregulation of NR1-1a isoform and an upregulation of NR1-3a isoform was observed in our transcriptomic analysis. However, we did not observe any significant changes in NR1(1-4)a isoforms by RT-PCR after the treatment. This apparent discordance could be explained by similar global expression levels of NR1(1-4)a isoforms, probably due to a compensatory mechanism between the up- (NR1-3a) and downregulation (NR1-1a) of both NR1(1-4)a isoforms, as suggested from the transcriptomic data. Surprisingly, NR1 isoforms were not modulated in the hippocampus of female mice, which opens the search for sexually dimorphic mechanisms of AM6545 treatment in memory modulation.

Our electrophysiological studies confirmed that sub-chronic AM6545 treatment increased the amplitude of EPSCs in the hippocampal CA1 region. As the experiments were performed at -70 mV, EPSCs were basically mediated by the activation of AMPA receptors. No changes in PPR were observed after AM6545 treatment, mainly discarding a presynaptic component in the facilitation of neurotransmitter release, and suggesting a postsynaptic increase in AMPA receptor-mediated currents. In this region, the activation of β-adrenergic receptors can trigger the phosphorylation of AMPAR facilitating their

traffic to extrasynaptic sites (Joiner et al., 2010; Rouach et al., 2005; Vanhoose & Winder, 2003) and reinforcing LTP (Oh et al., 2006), an explanation parsimonious with our experimental observations.

The neuronal plasticity changes elicited by AM6545 repeated administration could be also mediated by the increase of mRNA level of the neurotrophins *Bdnf* and *Ngf* in the hippocampus of AM6545-treated mice and a concomitant increase of BDNF protein levels. These neurotrophins have an important role in the regulation of long-term synaptic plasticity and memory (Gibon & Barker, 2017). Remarkably, an impairment of the BDNF signalling pathway leads to a downregulation of early and late phases of LTP in the Schaffer Collateral-CA1 hippocampal synapses and has been reported to hamper memory consolidation and reconsolidation (Bekinschtein et al., 2007; Korte et al., 1995). We also evaluated neuronal progenitor proliferation as a potential mechanism involved in synaptic plasticity changes. Previous evidence linked adult neurogenesis on the subgranular zone of the dentate gyrus to the establishment of hippocampal-dependent memory (Dupret et al., 2008; Jessberger et al., 2009; Saxe et al., 2006), and noradrenaline has been established to be a facilitator of cell proliferation in the hippocampus (Masuda et al., 2012). However, sub-chronic AM6545 treatment did not modify the number of cells expressing the cell proliferation marker Ki67 in this brain region, indicating that AM6545 is not modifying synaptic plasticity by altering hippocampal neurogenesis.

Altogether, our study suggests that sub-chronic peripheral CB1R inhibition contributes to the enhanced performance of low arousal and emotional memory persistence as well as executive function. These behavioural outcomes may be mediated by different hippocampal synaptic plasticity changes downstream of the noradrenergic signaling, mimicking to some extent the effects of systemic approaches reducing CB1R function

and pointing to the peripheral CB1R as a potential target to treat conditions associated to memory impairment.

Acknowledgements

We are grateful to Marta Linares, Raquel Martín and Francisco Porrón for expert technical assistance and the Laboratori de Neurofarmacologia-NeuroPhar for helpful discussion.

Funding and disclosure

A.B.-M. was supported by predoctoral fellowship from Spanish Ministry of Universities (FPU20/02061). L.R.-R. was supported by a predoctoral fellowship from Spanish Ministry of Science and Innovation (#PRE2019-087644). This work was supported by the Spanish Ministry of Science and Innovation (PID2021-123482OB-I00) to A.O, Generalitat de Catalunya, AGAUR (2021 SGR 00912) to R.M, the Spanish Agencia Estatal de Investigación (PID2019-107677GB-I00 and PID2022-136597NB-I00) and the Junta de Andalucía (P20-0881) to A.R.-M.

Conflict of interest statement

The authors declare that no conflict of interest exists.

References

Arguello, P. A., & Jentsch, J. D. (2004). Cannabinoid CB1 receptor-mediated impairment of visuospatial attention in the rat. *Psychopharmacology*, *177*(1–2), 141–150.

Barna, I., Soproni, K., Arszovszki, A., Csabai, K., & Haller, J. (2007). WIN-55,212-2 chronically implanted into the CA3 region of the dorsal hippocampus impairs learning: a novel method for studying chronic, brain-area-specific effects of cannabinoids. *Behavioural Pharmacology*, *18*(5–6), 515–520.

Bekinschtein, P., Cammarota, M., Igaz, L. M., Bevilaqua, L. R. M., Izquierdo, I., & Medina, J. H. (2007). Persistence of Long-Term Memory Storage Requires a Late Protein Synthesis- and BDNF- Dependent Phase in the Hippocampus. *Neuron*, *53*(2), 261–277.

Butler, C. W., Keiser, A. A., Kwapis, J. L., Berchtold, N. C., Wall, V. L., Wood, M. A., & Cotman, C. W. (2019). Exercise opens a temporal window for enhanced cognitive improvement from subsequent physical activity. *Learning & Memory*, *26*(12), 485.

Da Silva, G. E., & Takahashi, R. N. (2002). SR 141716A prevents Δ9-tetrahydrocannabinol-induced spatial learning deficit in a Morris-type water maze in mice. *Progress in Neuro-Psychopharmacology and Biological Psychiatry*, *26*(2), 321–325.

Dupret, D., Revest, J.-M., Koehl, M., Ichas, F., De Giorgi, F., Costet, P., Abrous, D. N., & Piazza, P. V. (2008). Spatial relational memory requires hippocampal adult neurogenesis. *PloS One*, *3*(4), e1959.

Falcón-Moya, R., Martínez-Gallego, I., & Rodríguez-Moreno, A. (2021). Kainate receptor modulation of glutamatergic synaptic transmission in the CA2 region of the hippocampus. *Journal of Neurochemistry*, *158*(5), 1083–1093.

Flores-Soto, M., Chaparro-Huerta, V., Escoto-Delgadillo, M., Elisa Ureña-Guerrero, M., Camins, A., & Beas-Zarate, C. (2013). Receptor to Glutamate NMDA-Type: The Functional Diversity of the NR1 Isoforms and Pharmacological Properties. *Current Pharmaceutical Design*, *19*(38), 6709–6719.

Gibon, J., & Barker, P. A. (2017). Neurotrophins and Proneurotrophins: Focus on Synaptic Activity and Plasticity in the Brain. *The Neuroscientist*, *23*(6), 587–604.

Hafner, A. S., Donlin-Asp, P. G., Leitch, B., Herzog, E., & Schuman, E. M. (2019). Local protein synthesis is a ubiquitous feature of neuronal pre- and postsynaptic compartments. *Science (New York, N.Y.)*, *364*(6441).

Horner, A. E., Heath, C. J., Hvoslef-Eide, M., Kent, B. A., Kim, C. H., Nilsson, S. R. O., Alsiö, J., Oomen, C. A., Holmes, A., Saksida, L. M., & Bussey, T. J. (2013). The touchscreen operant platform for testing learning and memory in rats and mice. *Nature Protocols*, *8*(10), 1961–1984.

Ishac, E. J. N., Jiang, L., Lake, K. D., Varga, K., Abood, M. E., & Kunos, G. (1996). Inhibition of exocytotic noradrenaline release by presynaptic cannabinoid CB1 receptors on peripheral sympathetic nerves. *British Journal of Pharmacology*, *118*(8), 2023–2028.

Jessberger, S., Clark, R. E., Broadbent, N. J., Clemenson, G. D., Consiglio, A., Lie, D. C., Squire, L. R., & Gage, F. H. (2009). Dentate gyrus-specific knockdown of adult neurogenesis impairs spatial and object recognition memory in adult rats. *Learning & Memory*, *16*(2), 147–154.

Joiner, M. A., Lisé, M.-F., Yuen, E. Y., Kam, A. Y. F., Zhang, M., Hall, D. D., Malik, Z. A., Qian, H., Chen, Y., Ulrich, J. D., Burette, A. C., Weinberg, R. J., Law, P.-Y., El-Husseini, A., Yan, Z., & Hell, J. W. (2010). Assembly of a beta2-adrenergic receptor--GluR1 signalling complex for localized cAMP signalling. *The EMBO Journal*, *29*(2), 482–495.

Kilkenny, C., Browne, W., Cuthill, I. C., Emerson, M., Altman, D. G., & NC3Rs Reporting Guidelines Working Group. (2010). Animal research: Reporting in vivo experiments: The ARRIVE guidelines. *British Journal of Pharmacology*, *160*(7), 1577–1579.

King, S. O., & Williams, C. L. (2009). Novelty-induced arousal enhances memory for cued classical fear conditioning: Interactions between peripheral adrenergic and brainstem glutamatergic systems. *Learning & Memory*, *16*(10), 625–634.

Korte, M., Carroll, P., Wolf, E., Brem, G., Thoenen, H., & Bonhoeffer, T. (1995). Hippocampal

long-term potentiation is impaired in mice lacking brain-derived neurotrophic factor. *Proceedings of the National Academy of Sciences*, *92*(19), 8856–8860.

Kruk-Slomka, M., & Biala, G. (2016). CB1 receptors in the formation of the different phases of memory-related processes in the inhibitory avoidance test in mice. *Behavioural Brain Research*, *301*, 84–95.

Lau, C. G., & Zukin, R. S. (2007). NMDA receptor trafficking in synaptic plasticity and neuropsychiatric disorders. *Nature Reviews Neuroscience 2007 8:6*, *8*(6), 413–426.

Livak, K. J., & Schmittgen, T. D. (2001). Analysis of Relative Gene Expression Data Using Real-Time Quantitative PCR and the 2−ΔΔCT Method. *Methods*, *25*(4), 402–408.

Love, M. I., Huber, W., & Anders, S. (2014). Moderated estimation of fold change and dispersion for RNA-seq data with DESeq2. *Genome Biology*, *15*(12), 550.

Maccarrone, M., Valverde, O., Barbaccia, M. L., Castañé, A., Maldonado, R., Ledent, C., Parmentier, M., & Finazzi-Agrò, A. (2002). Age-related changes of anandamide metabolism in CB1 cannabinoid receptor knockout mice: correlation with behaviour. *The European Journal of Neuroscience*, *15*(7), 1178–1186.

Marsicano, G., Wotjak, C. T., Azad, S. C., Bisogno, T., Rammes, G., Cascioll, M. G., Hermann, H., Tang, J., Hofmann, C., Zieglgänsberger, W., Di Marzo, V., & Lutz, B. (2002). The endogenous cannabinoid system controls extinction of aversive memories. *Nature*, *418*(6897), 530–534.

Martínez-Torres, S., Bergadà-Martínez, A., Ortega, J. E., Galera-López, L., Hervera, A., de los Reyes-Ramírez, L., Ortega-Álvaro, A., Remmers, F., Muñoz-Moreno, E., Soria, G., del Río, J. A., Lutz, B., Ruíz-Ortega, J. Á., Meana, J. J., Maldonado, R., & Ozaita, A. (2023). Peripheral CB1 receptor blockade acts as a memory enhancer through a noradrenergic mechanism. *Neuropsychopharmacology*, *48*(2), 341–350.

Masuda, T., Nakagawa, S., Boku, S., Nishikawa, H., Takamura, N., Kato, A., Inoue, T., & Koyama, T. (2012). Noradrenaline increases neural precursor cells derived from adult rat dentate gyrus through beta2 receptor. *Progress in Neuro-Psychopharmacology and Biological Psychiatry*, *36*(1), 44–51.

McIntyre, C. K., McGaugh, J. L., & Williams, C. L. (2012). Interacting brain systems modulate memory consolidation. *Neuroscience & Biobehavioral Reviews*, *36*(7), 1750–1762.

Morris, R. G. M. (2006). Elements of a neurobiological theory of hippocampal function: the role of synaptic plasticity, synaptic tagging and schemas. *The European Journal of Neuroscience*, *23*(11), 2829–2846.

Navarro-Romero, A., Galera-López, L., Ortiz-Romero, P., Llorente-Ovejero, A., de los Reyes-Ramírez, L., de Tena, I. B., Garcia-Elias, A., Mas-Stachurska, A., Reixachs-Solé, M., Pastor, A., de la Torre, R., Maldonado, R., Benito, B., Eyras, E., Rodríguez-Puertas, R., Campuzano, V., & Ozaita, A. (2022). Cannabinoid signaling modulation through JZL184 restores key phenotypes of a mouse model for Williams-Beuren syndrome. *ELife*, *11*, e72560.

Navarro-Romero, A., Vázquez-Oliver, A., Gomis-González, M., Garzón-Montesinos, C., Falcón-Moya, R., Pastor, A., Martín-García, E., Pizarro, N., Busquets-Garcia, A., Revest, J. M., Piazza, P. V., Bosch, F., Dierssen, M., de la Torre, R., Rodríguez-Moreno, A., Maldonado, R., & Ozaita, A. (2019). Cannabinoid type-1 receptor blockade restores neurological phenotypes in two models for Down syndrome. *Neurobiology of Disease*, *125*, 92–106.

Niederhoffer, N., Hansen, H. H., Fernandez-Ruiz, J. J., & Szabo, B. (2001). Effects of cannabinoids on adrenaline release from adrenal medullary cells. *British Journal of Pharmacology*, *134*(6), 1319–1327.

Oh, M. C., Derkach, V. A., Guire, E. S., & Soderling, T. R. (2006). Extrasynaptic Membrane Trafficking Regulated by GluR1 Serine 845 Phosphorylation Primes AMPA Receptors for Long-term Potentiation. *Journal of Biological Chemistry*, *281*(2), 752–758.

Ohno-Shosaku, T., & Kano, M. (2014). Endocannabinoid-mediated retrograde modulation of synaptic transmission. *Current Opinion in Neurobiology*, *29*, 1–8.

Pacher, P., Bátkai, S., & Kunos, G. (2006). The Endocannabinoid System as an Emerging Target of Pharmacotherapy. *Pharmacological Reviews*, *58*(3), 389–462.

Pamplona, F. A., & Takahashi, R. N. (2006). WIN 55212-2 impairs contextual fear conditioning

through the activation of CB1 cannabinoid receptors. *Neuroscience Letters*, *397*(1–2), 88–92.

Paoletti, P., Bellone, C., & Zhou, Q. (2013). *NMDA receptor subunit diversity: impact on receptor properties, synaptic plasticity and disease*.

Patro, R., Duggal, G., Love, M. I., Irizarry, R. A., & Kingsford, C. (2017). Salmon: fast and bias-aware quantification of transcript expression using dual-phase inference. *Nature Methods*, *14*(4), 417.

Pérez-Rodríguez, M., Arroyo-García, L. E., Prius-Mengual, J., Andrade-Talavera, Y., Armengol, J. A., Pérez-Villegas, E. M., Duque-Feria, P., Flores, G., & Rodríguez-Moreno, A. (2019). Adenosine Receptor-Mediated Developmental Loss of Spike Timing-Dependent Depression in the Hippocampus. *Cerebral Cortex (New York, N.Y. : 1991)*, *29*(8), 3266–3281.

Puighermanal, E., Marsicano, G., Busquets-Garcia, A., Lutz, B., Maldonado, R., & Ozaita, A. (2009). Cannabinoid modulation of hippocampal long-term memory is mediated by mTOR signaling. *Nature Neuroscience*, *12*(9), 1152–1158.

Reibaud, M., Obinu, M. C., Ledent, C., Parmentier, M., Böhme, G. A., & Imperato, A. (1999). Enhancement of memory in cannabinoid CB1 receptor knock-out mice. *European Journal of Pharmacology*, *379*(1), R1-2.

Roozendaal, B., McEwen, B. S., & Chattarji, S. (2009). Stress, memory and the amygdala. *Nature Reviews. Neuroscience*, *10*(6), 423–433.

Rouach, N., Byrd, K., Petralia, R. S., Elias, G. M., Adesnik, H., Tomita, S., Karimzadegan, S., Kealey, C., Bredt, D. S., & Nicoll, R. A. (2005). TARP γ-8 controls hippocampal AMPA receptor number, distribution and synaptic plasticity. *Nature Neuroscience*, *8*(11), 1525–1533.

Salgado-Mendialdúa, V., Aguirre-Plans, J., Guney, E., Reig-Viader, R., Maldonado, R., Bayés, Oliva, B., & Ozaita, A. (2018). Δ9-tetrahydrocannabinol modulates the proteasome system in the brain. *Biochemical Pharmacology*, *157*, 159–168.

Saxe, M. D., Battaglia, F., Wang, J.-W., Malleret, G., David, D. J., Monckton, J. E., Garcia, A. D. R., Sofroniew, M. V., Kandel, E. R., Santarelli, L., Hen, R., & Drew, M. R. (2006). Ablation of hippocampal neurogenesis impairs contextual fear conditioning and synaptic plasticity in the dentate gyrus. *Proceedings of the National Academy of Sciences*, *103*(46), 17501–17506.

Sengar, A. S., Li, H., Zhang, W., Leung, C., Ramani, A. K., Saw, N. M., Wang, Y., Tu, Y. S., Ross, P. J., Scherer, S. W., Ellis, J., Brudno, M., Jia, Z., & Salter, M. W. (2019). Control of Long-Term Synaptic Potentiation and Learning by Alternative Splicing of the NMDA Receptor Subunit GluN1. *Cell Reports*, *29*(13), 4285-4294.e5.

Soneson, C., Love, M. I., & Robinson, M. D. (2016). Differential analyses for RNA-seq: transcript-level estimates improve gene-level inferences. *F1000Research 2016 4:1521*, *4*, 1521.

Takahashi, R. N., Pamplona, F. A., & Fernandes, M. S. (2005). The cannabinoid antagonist SR141716A facilitates memory acquisition and consolidation in the mouse elevated T-maze. *Neuroscience Letters*, *380*(3), 270–275.

Terranova, J. P., Storme, J. J., Lafon, N., Péŕio, A., Rinaldi-Carmona, M., Le Fur, G., & Soubrié, P. (1996). Improvement of memory in rodents by the selective CB1 cannabinoid receptor antagonist, SR 141716. *Psychopharmacology*, *126*(2), 165–172.

Vanhoose, A. M., & Winder, D. G. (2003). NMDA and beta1-adrenergic receptors differentially signal phosphorylation of glutamate receptor type 1 in area CA1 of hippocampus. *The Journal of Neuroscience : The Official Journal of the Society for Neuroscience*, *23*(13), 5827–5834.

Wolff, M. C., & Leander, J. D. (2003). SR141716A, a cannabinoid CB1 receptor antagonist, improves memory in a delayed radial maze task. *European Journal of Pharmacology*, *477*(3), 213–217.

Xu, X., Jiang, S., Xu, E., Wu, X., & Zhao, R. (2019). Inhibition of CB1 receptor ameliorates spatial learning and memory impairment in mice with traumatic brain injury. *Neuroscience Letters*, *696*, 127–131.

Yang, C., Liu, J.-F., Chai, B.-S., Fang, Q., Chai, N., Zhao, L.-Y., Xue, Y.-X., Luo, Y.-X., Jian, M., Han, Y., Shi, H.-S., Lu, L., Wu, P., & Wang, J.-S. (2013). Stress within a restricted time window selectively affects the persistence of long-term memory. *PloS One*, *8*(3), e59075.

Yu, G., Wang, L. G., Han, Y., & He, Q. Y. (2012). clusterProfiler: an R Package for Comparing Biological Themes Among Gene Clusters. *OMICS : A Journal of Integrative Biology*, *16*(5), 284.

Zanettini, C., Panlilio, L. V, Alicki, M., Goldberg, S. R., Haller, J., & Yasar, S. (2011). Effects of endocannabinoid system modulation on cognitive and emotional behavior. *Frontiers in Behavioral Neuroscience*, *5*, 57.

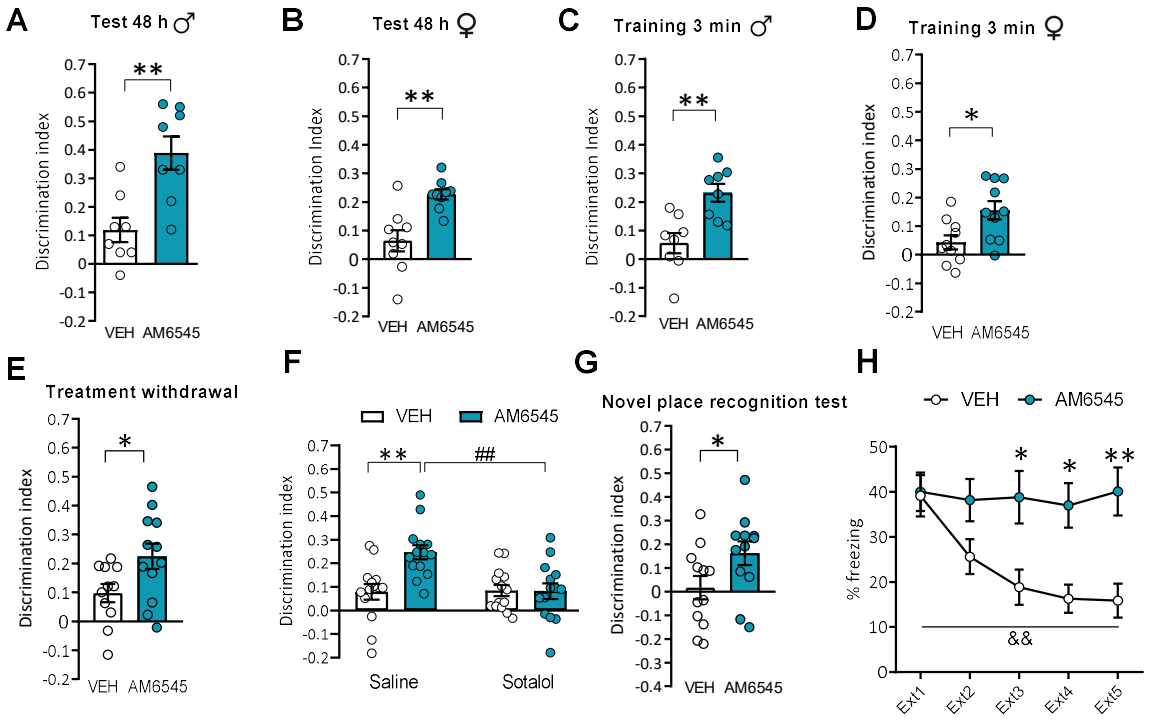

Figure 1. Sub-chronic AM6545 treatment improves both non-emotional and emotional memory. (**A,B)** Discrimination index values in NORT at 48 h after sub-chronic 7 days treatment with vehicle (VEH) or AM6545 (1 mg/kg) (n = 8-9) in both male (**A**) and female (**B**) mice**.** (**C,D)** Discrimination index values in NORT at 24 h after sub-chronic 7 d treatment with vehicle (VEH) or AM6545 (1 mg/kg) with a 3 min training period (n = 8-10**)** in both male **(C)** and female **(D)** mice**. (E)** Discrimination index values in NORT at 48 h after treatment withdrawal (n = 11-12). **(F)** Discrimination index values in NORT after sub-chronic 7 days treatment with vehicle (VEH) or AM6545 (1 mg/kg) after pretreatment with saline or sotalol (10 mg/kg) (n = 14). **(G)** Discrimination index values in NPRT at 48 h after sub-chronic 7 days treatment with vehicle (VEH) or AM6545 (1 mg/kg) (n = 12). **(H)** Percentage of freezing in the context fear conditioning across extinction sessions (Ext1-Ext5) after post-extinction 1-5 treatment with vehicle (VEH) or AM6545 (1 mg/kg) (n = 16). Data are expressed as mean ± s.e.m. * $p < 0.05$, ** $p < 0.01$ (treatment effect), ## $p < 0.01$ (pretreatment effect), && $p < 0.01$ (time effect) by Student's t-test or two-way repeated measures ANOVA followed by Bonferroni *post hoc*.

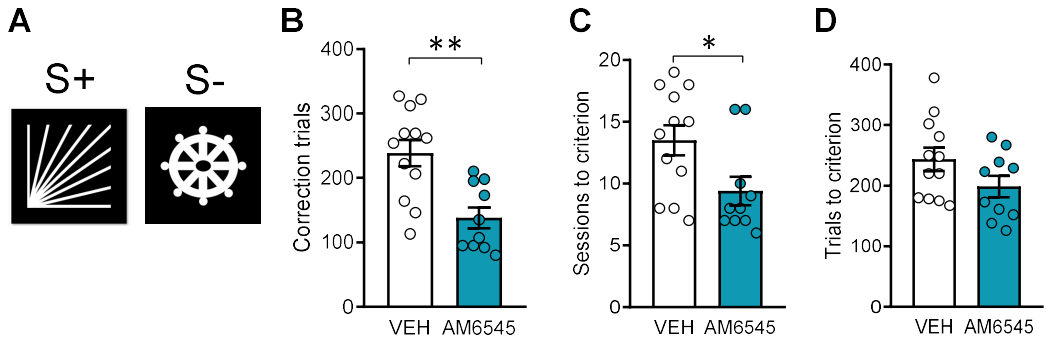

Figure 2. Long-term peripheral CB1R inhibition improves executive function in the pairwise discrimination task. (**A)** Image pair presented in the touchscreen during the pairwise discrimination test. (**B-D)** Total number of correction trials **(B)**, sessions **(C)** and trials **(D)** required to reach criterion in animals treated with vehicle (VEH) or AM6545 (1 mg/kg) (n = 10-12). Data are expressed as mean ± s.e.m. * $p <$ 0.05, ** $p < 0.01$ by Student's t-test.

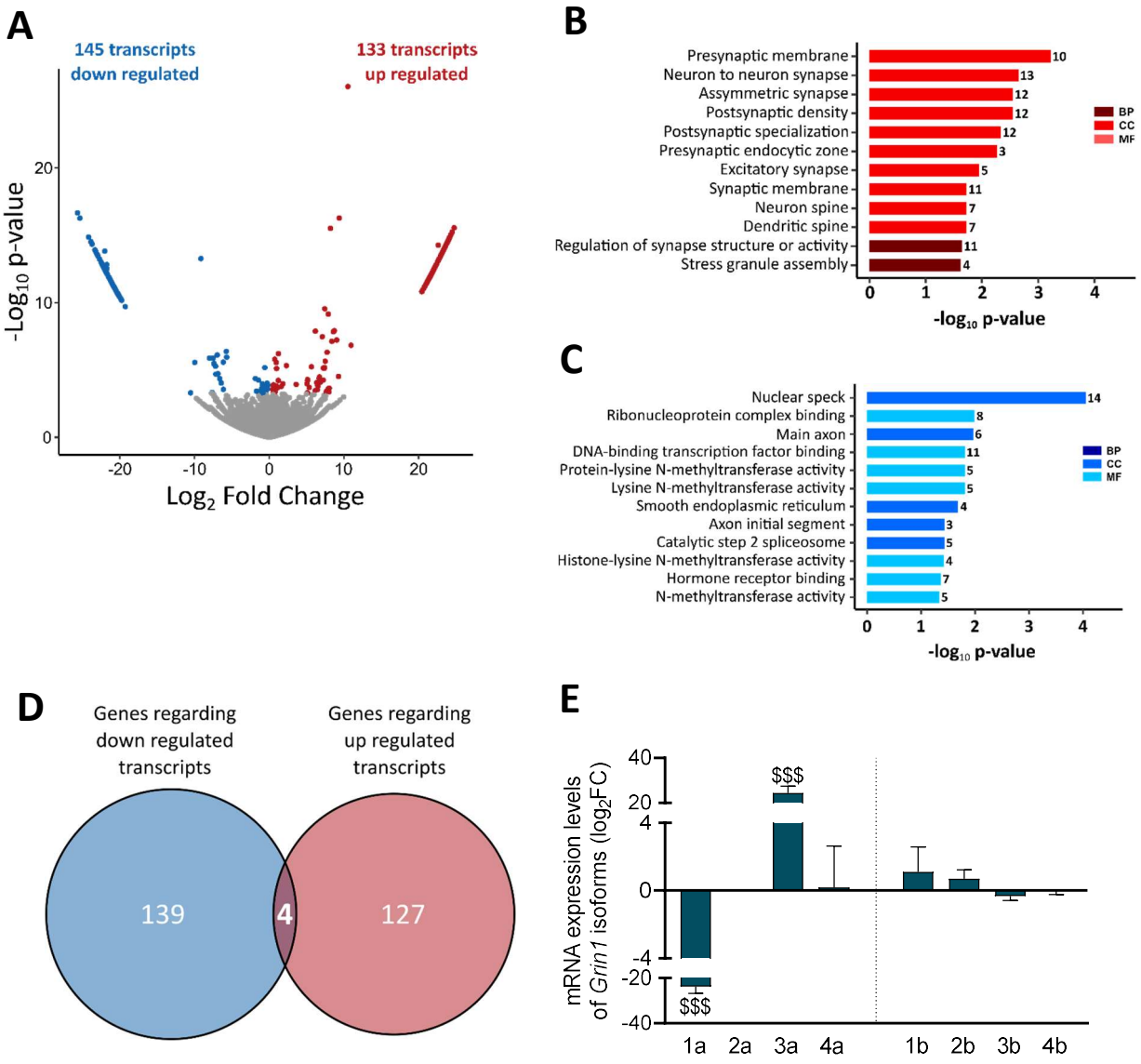

Figure 3. Sub-chronic peripheral CB1R inhibition modulates hippocampal transcripts expression. **(A)** Volcano plot of differentially expressed transcripts between vehicle and AM6545-treated mice. Red indicates significant up regulation ($p < 0.05$ and $log_2FC > 0$), blue significant downregulation ($p < 0.05$ and $log_2FC < 0$) and grey non-significant differential expression ($p \geq 0.05$). **(B, C)** Gene ontology enrichment analysis for both up- **(B)** and downregulated **(C)** genes associated to each transcript in AM6545-treated mice compared to vehicle. Most significant GO terms are represented, and colors indicates GO category of each term. BP: biological processes, MF: molecular function, CC: cellular component. **(D)** Venn diagram with genes associated to each transcript that were down- or upregulated after AM6545 administration. **(E)** Bar plot of relative mRNA expression of *Grin1* isoforms (mean log_2 fold change ± s.e.m.) in sub-chronic AM6545-treated mice compared to vehicle-treated mice (WT-VEH, $n = 5$; WT-AM6545, $n = 5$). Statistical significance was calculated by Benjamini-Hochberg adjustment following Wald test analysis. $$$ $p < 0.01$ (WT-AM6545 *vs.* WT-VEH).

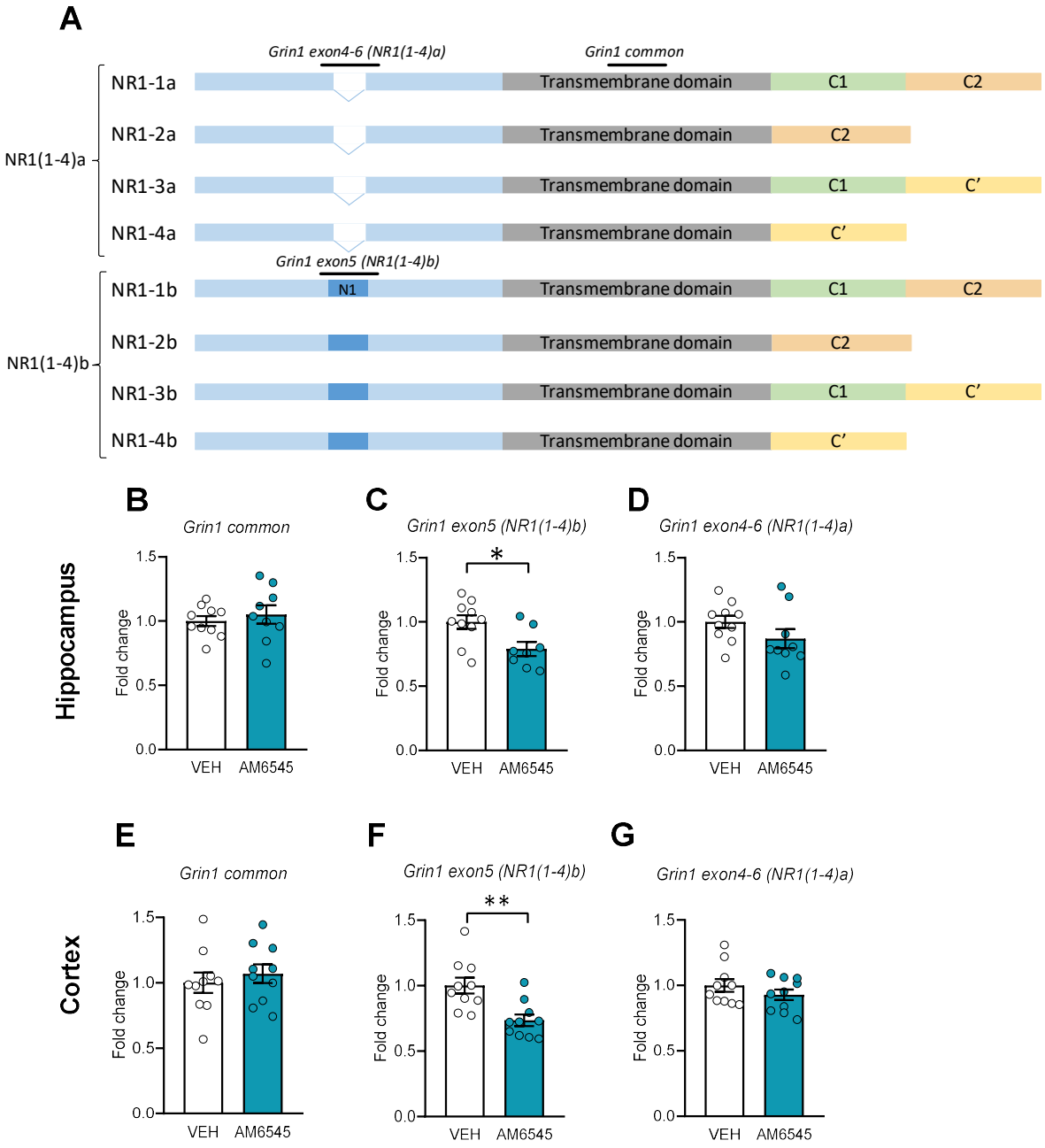

Figure 4. Sub-chronic AM6545 treatment modulates NR1 subunit isoforms both in the hippocampus and cortex. (A) Schematic representation of *Grin1* isoforms showing the transmembrane (common) domain and the N1, C1, C2 and C' cassettes. The primers used are indicated over the amplified region. **(B-D)** Hippocampal mRNA levels of NR1 isoforms *Grin1 common* **(B)**, *Grin1 exon5* **(C)**, *Grin1 exon4-6* **(D)** of mice treated for 7 days with vehicle (VEH) or AM6545 (1 mg/kg) (n = 8-10). **(E-G)** Cortical mRNA levels of NR1 isoforms *Grin1 common* **(E)**, *Grin1 exon5* **(F)**, *Grin1 exon4-6* **(G)** of mice treated for 7 days with vehicle (VEH) or AM6545 (1 mg/kg) (n = 10). Data are expressed as mean ± s.e.m. * $p < 0.05$, ** $p < 0.01$, by Student's t-test.

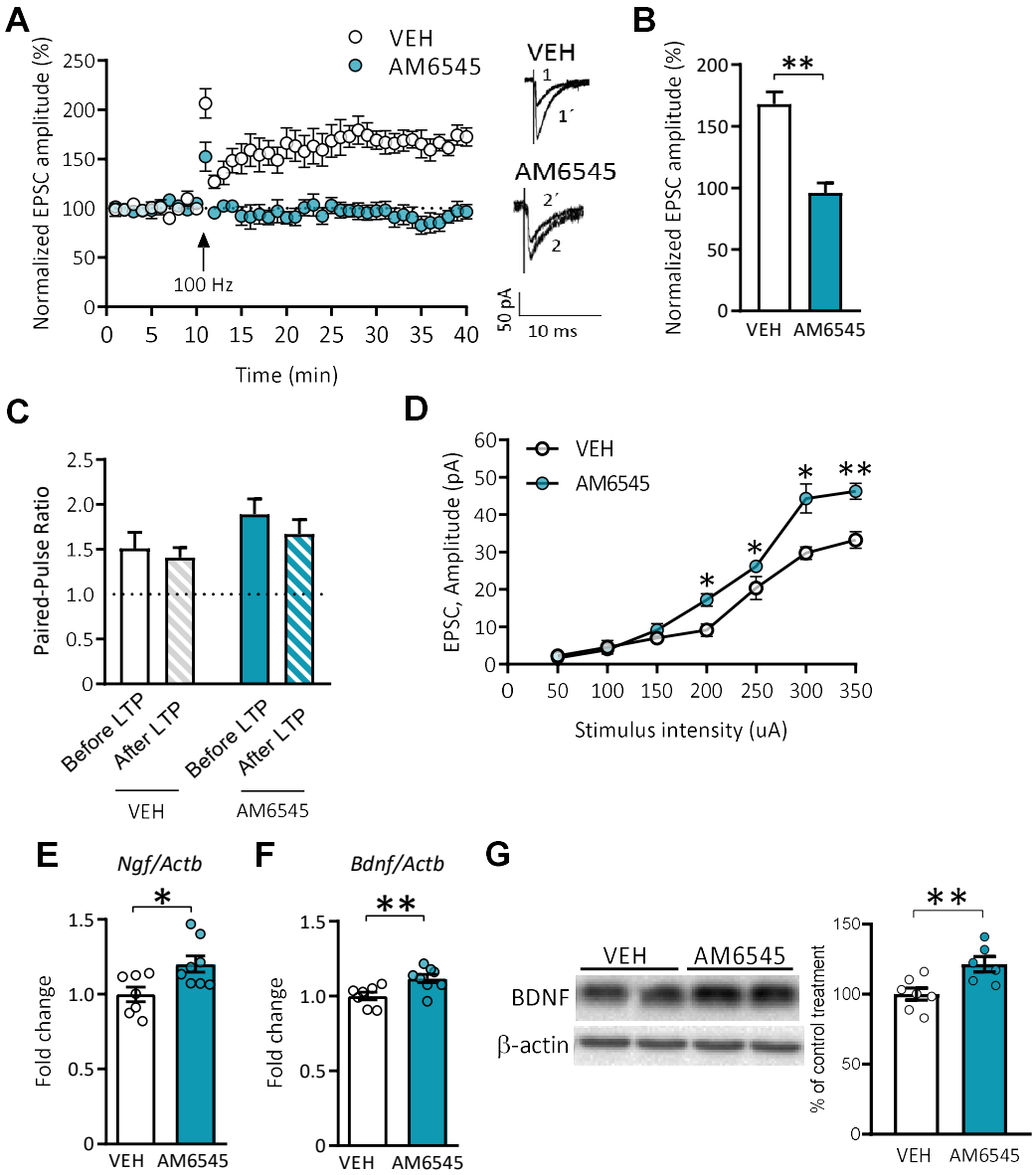

Figure 5. Sub-chronic peripheral CB1R inhibition enhances synaptic plasticity in the hippocampus. **(A)** Average time courses of the change in the amplitude of the EPSC in hippocampal slices from mice treated for 7 days with vehicle (VEH) or AM6545 (1 mg/kg). Traces represent samples of EPSC. recorded for each experimental group before (1,2) and 30 min after (1',2') LTP induction (n = 6). **(B)** Average LTP of the last 5 min of recordings (n = 6). **(C)** Paired-pulse ratio before and after (fill pattern bars) LTP induction in hippocampal slices from mice treated for 7 days with vehicle (VEH) or AM6545 (1 mg/kg). **(D)** Stimulation input/output curves in hippocampal slices from mice treated for 7 d with vehicle (VEH) or AM6545 (1 mg/kg). **(E,F)** Hippocampal mRNA levels of the neurotrophic factors *Ngf* **(E)** and *Bdnf* **(F)** of mice treated for 7 days with vehicle (VEH) or AM6545 (1 mg/kg) (n = 7 - 8). **(G)** Representative immunoblot and quantification of BDNF total expression in the hippocampus of mice treated for 7 days with vehicle (VEH) or AM6545 (1 mg/kg) (n = 7). Data are expressed as mean ± s.e.m. * $p < 0.05$, ** $p < 0.01$ by Student's t-test or two-way repeated measures ANOVA followed by Bonferroni *post hoc*.

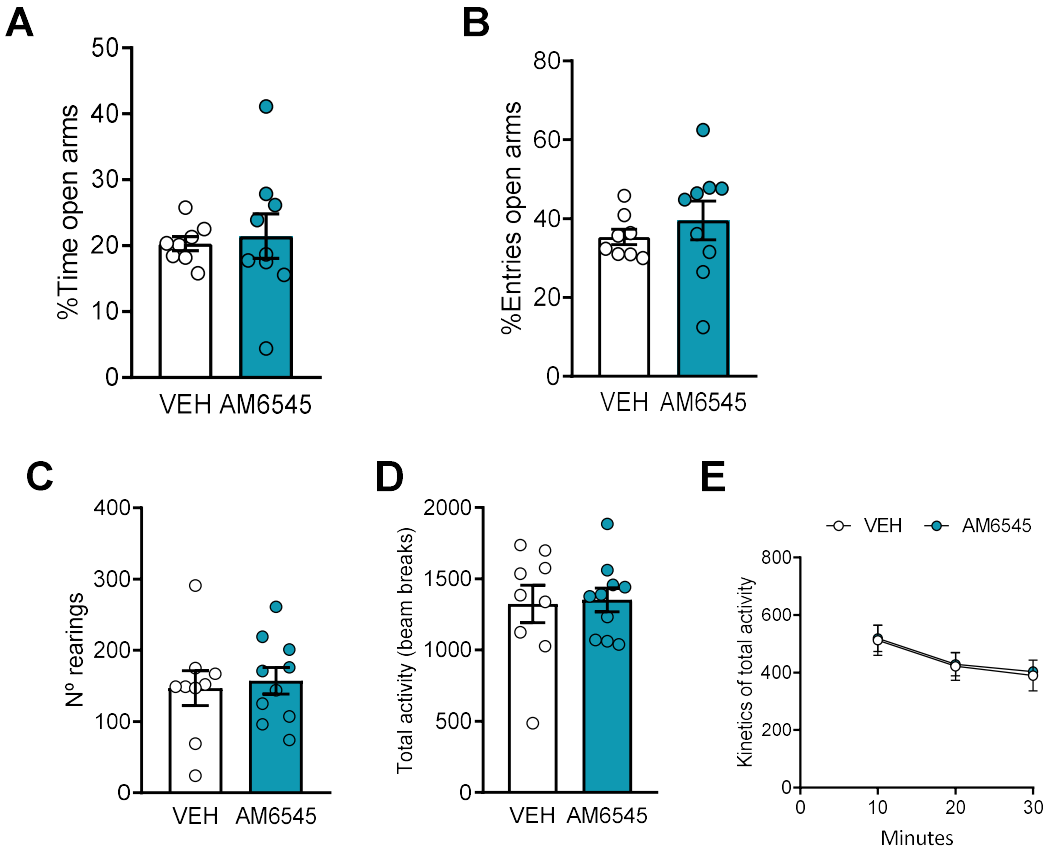

Supplementary Figure 1. Sub-chronic AM6545 treatment does not modify anxiety-like behavior and locomotor activity. (A,B) Percentage of time **(A)** and entries **(B)** to the open arms in the elevated-plus maze test after sub-chronic 7 days treatment with vehicle (VEH) or AM6545 (1 mg/kg) (n = 8 – 9). **(C-E)** Total number of rearings **(C)**, total activity **(D)** and kinetics of total activity **(E)** during 30 min after sub-chronic 7 days treatment with vehicle (VEH) or AM6545 (1 mg/kg) (n = 9 – 10). Data are expressed as mean ± s.e.m. Statistical significance was calculated by Student's t test or two-way repeated measures ANOVA.

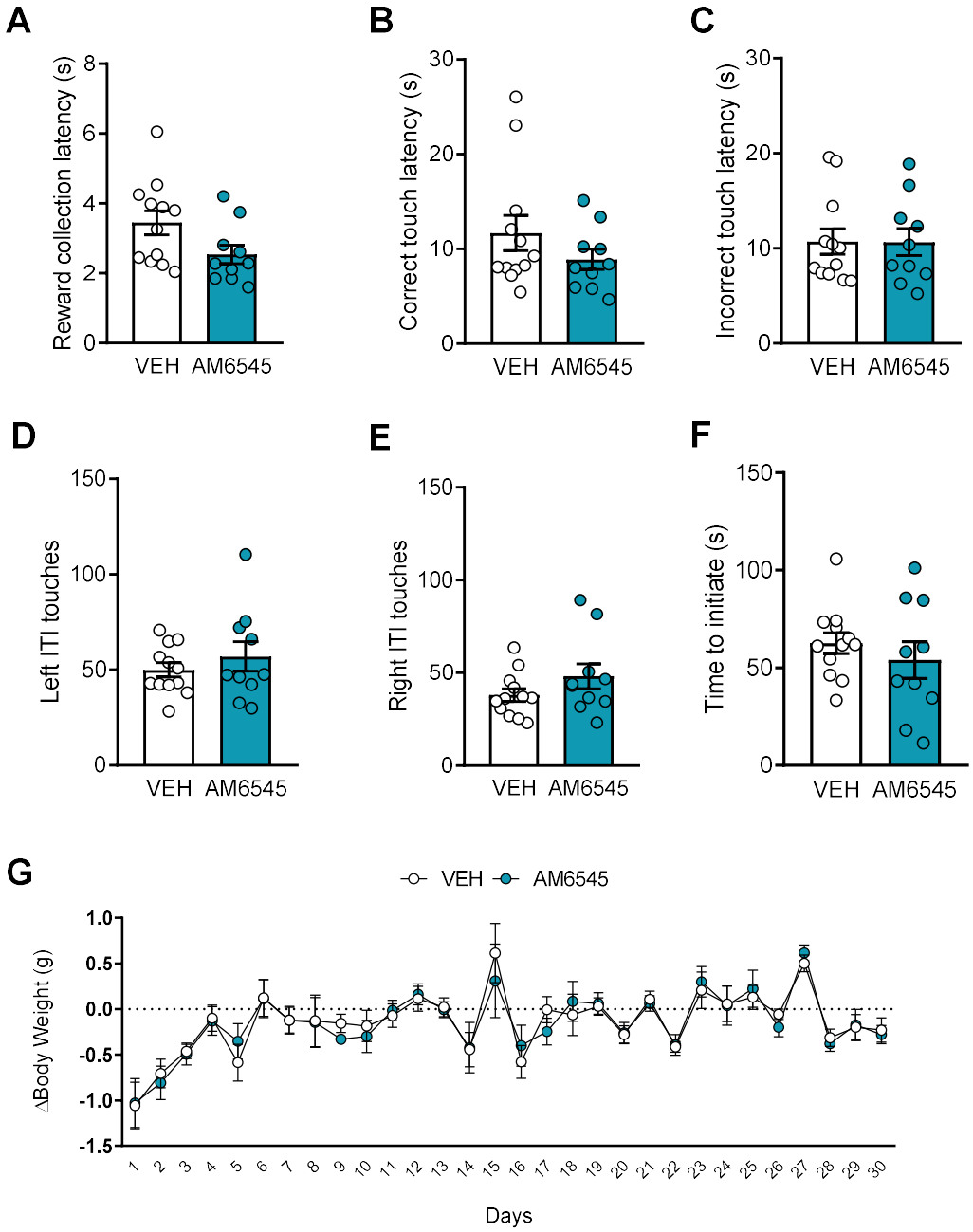

Supplementary Figure 2. Long-term peripheral CB1R inhibition does not modify control parameters or body weight in the pairwise discrimination task. (**A-F)** Reward collection latency (**A**), correct (**B**) and incorrect (**C**) touch latency, left (**D**) and right (**E**) ITI touches and time to initiate the trials (**F**) in animals treated with vehicle (VEH) or AM6545 (1 mg/kg) (n = 12-14). (**G**) Weight variation between days in animals treated with vehicle (VEH) or AM6545 (1 mg/kg) (n = 12-14). Data are expressed as mean ± s.e.m. Statistical significance was calculated by Student's t-test or two-way ANOVA.

Gene ID	Gene name	log_2FC	lfcSE	p-value	Adjusted p-value
ENSMUSG00000038495	*Otud7b*	0.5499	0.1270	1.49E-05	0.067
ENSMUSG00000039985	*Sinhcaf*	-1.2712	0.2763	4.21E-06	0.025
ENSMUSG00000047793	*Sned1*	-1.2058	0.2871	2.66E-05	0.096
ENSMUSG00000095675	*Ccl21b*	-21.3809	3.0285	1.67E-12	1.51E-08
ENSMUSG00000109941	*Exosc6*	-21.6889	3.0280	7.91E-13	1.43E-08

Supplementary Figure 3. Sub-chronic AM6545 administration only modifies few hippocampal genes. Summary of differentially expressed genes in hippocampal synaptoneurosomes from mice treated with AM6545 compared to mice treated with vehicle. Threshold for significance was settled at adjusted p-value < 0.1. (WT-VEH, n = 5; WT-AM6545, n = 5). Statistical significance was calculated by Benjamini-Hochberg adjustment following Wald test analysis.

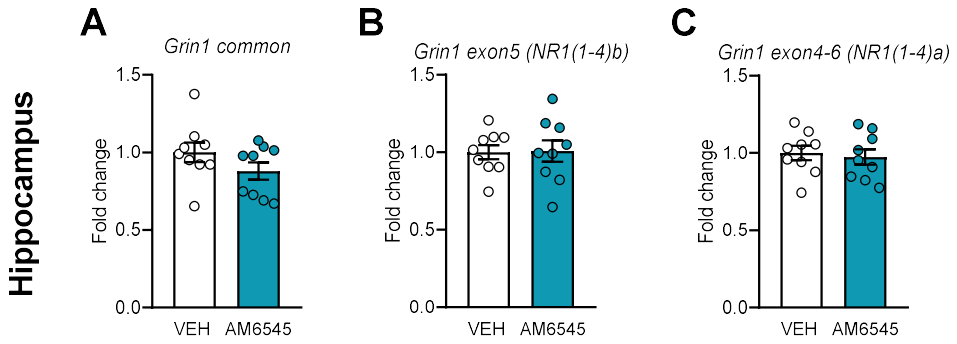

Supplementary Figure 4. Sub-chronic AM6545 treatment does not modulate NR1 subunit isoforms in the hippocampus from female mice. (A-C) Hippocampal mRNA levels of NR1 isoforms *Grin1 common* **(A)**, *Grin1 exon5* **(B)** and *Grin1 exon4-6* **(C)** of mice treated for 7 days with vehicle (VEH) or AM6545 (1 mg/kg) (n = 9). Data are expressed as mean ± s.e.m. Statistical significance was calculated by Student's t-test.

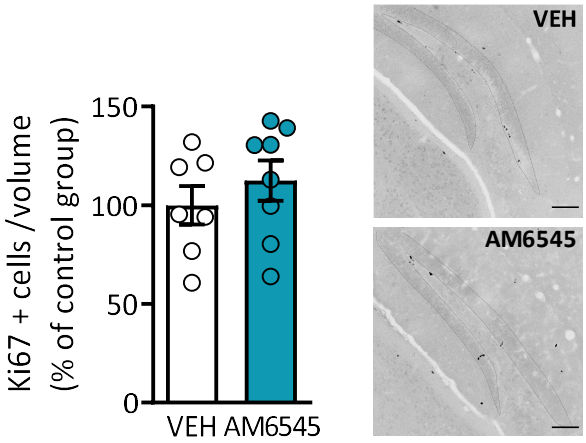

Supplementary Figure 5. Sub-chronic peripheral CB1R inhibition does not modify hippocampal neurogenesis. Average density of Ki67+ cells and representative greyscale confocal images in the subgranular zone of the dentate gyrus of mice treated for 7 days with vehicle (VEH) AM6545 (1 mg/kg) (*n* = 7 - 8**)** (scale bar = 100 µm**).** Data are expressed as mean ± s.e.m. Statistical significance was calculated by Student's t-test.